

Determination of Metandienone using molecularly Imprinted based Electrochemical Sensor in human urine

Juan Bao^{1,*}, Qing Zhang¹, Wei Huang²

¹ Physical Education College of Zaozhuang University, Zaozhuang, 277100, China

² School of chemistry, chemical engineering and materials science, Zaozhuang University, Zaozhuang, 277100, China

*CorrespondingE-mail: bao197809@sina.com

Received: 22 August 2022 / Accepted: 5 October 2022 / Published: 17 November 2022

The current study sought to develop a molecularly imprinted polymer and graphene oxide nanocomposite on glassy carbon electrode (MIP/GO/GCE) as an electrochemical sensor for the selective detection of metandienone (MD) as a doping agent in wrestler biological fluid samples. The MIP/GO nanocomposite on GCE was created using an electropolymerization technique. FE-SEM and XRD structural and morphological studies confirmed the successful electropolymerization of MIP on GO nanosheets in the MIP/GO nanocomposite which modified the GCE surface. Due to the synergistic effect of GO and MIPs, electrochemical measurements using DPV and amperometry techniques revealed highly selective MD determination and significantly enhanced electrocatalytic activity of MIP/GO nanocomposite. MIP/GO/GCE linear response was measured from 0 to 2900 ng/mL. The sensitivity and detection limit were calculated to be $0.01967\mu\text{A}/\text{ng}\cdot\text{mL}^{-1}$ and 0.07ng/mL, respectively. Furthermore, when compared to the released outcomes of MD sensors in literatures, MIP/GO/GCE demonstrated significant electrocatalytic performance with a broad linear range to MD concentrations and an appropriate limit of detection value. The MIP/GO/GCE sensing system was evaluated as a proposed sensing system for MD analysis in real samples prepared from wrestler urine. Analytical studies revealed that the RSD values (3.15% to 4.73%) were suitable for valid and accurate practical analyses in urine and other biological fluid samples.

Keywords: Graphene Oxide, Molecularly *Imprinted* Polymers; Specificity; Electropolymerization; Metandienone; Wrestlers; Amperometry

1. INTRODUCTION

Metandienone (MD), also known as methandienone or methandrostenolone and sold under the brand name Dianabol as anabolic steroids, is most commonly used by competitive athletes, bodybuilders, wrestlers, and powerlifters for physique and performance enhancement [1, 2]. MD is a

drug that has androgenic activity, which means it has the ability to increase muscle mass, leg performance, strength, and tone [3, 4]. MD is ideal for mass gain because it rapidly increases muscle size and strength. It also increases protein levels in the muscles, which aids in muscle growth and recovery [5, 6]. MD is also effective at stimulating muscle growth. MD is on the WADA Prohibited List from 2006. Furthermore, MD has a slew of negative side effects that can harm both men and women [7, 8]. Gynecomastia (male breast enlargement), acne, increased aggression, heart problems, liver damage, and stroke are the most common side effects of MD [9]. Furthermore, excessive MD use can raise cholesterol levels, reduce sperm count in men, and cause infertility in women. Other MD side effects in bodybuilding include insomnia, nausea, vomiting, muscle cramps, and high blood pressure [10-12].

Spectrophotometry [13], mass spectrometry [14], capillary electrophoresis process [15], gas chromatography-mass spectrometry (GC-MS) [16], gas chromatography–low-resolution mass spectrometry with selected ion monitoring (GC–LRMS–SIM) [17], liquid chromatography tandem mass spectrometry (LC–MS/MS) [18], enzyme-linked immunosorbent assay (ELISA) [19] and electrochemical techniques [20-22] have all been used to determine MD concentration in pharmaceutical and biological fluids samples. One of the most difficult drawbacks of these methods is signal suppression due to fouling agents and interference from chemicals present in the sample matrix, indicating low selectivity [23, 24]. According to research, molecular imprinting technology is a technique for creating molecularly imprinted polymers (MIPs) with tailor-made binding sites that are complementary to the template molecules in shape, size, and functional groups [25, 26]. It can be described as a method of creating a molecular lock to match a molecular key, with the specificity determined by functional group complementarity as well as the shape of the binding cavity in MIPs [27, 28]. Thus, the current study aims to develop a GO and MIP-based electrochemical sensor for the selective detection of MD as a doping agent in athlete biological fluid samples.

2. EXPERIMENT

2.1. Fabrication of MIP/GO nanocomposite modified the GCE surface

Electropolymerization technique was used for fabrication of MIP/GO nanocomposite modified the GCE surface [29, 30]. To achieve a mirror-like surface, GCE (diameter 3 mm) was polished with 1 m and 3 m aluminum oxide slurry (99.99%, Zibo Linxi Chemical Co., Ltd., China) on a Buehler Microcloth® pad. After polishing, the GCE was ultrasonically rinsed in deionized water for 8 minutes and sonicated for 5 minutes in anhydrous ethanol (99%, Duter Co., Ltd., China). 2 mg of GO (99%, Sigma-Aldrich) was homogeneously dispersed in 50 mL of dimethylformamide (DMF, 99.9%, Shandong Near Chemical Co., Ltd., China) prior to electropolymerization. To obtain GO/GCE, 100 L of the GO-DMF suspension was dropped on the GCE surface and dried under an infrared lamp. Electropolymerization was carried out at 0.7 V for 4 minutes using an electrochemical workstation potentiostat (RRDE-6A, Taizhou Hervey Instrument Co., Ltd., Jiangsu, China) in a three-electrode system containing a working electrode (GO/GCE), a counter electrode (platinum mesh), and a

reference electrode (Ag/AgCl (3 M KCl)). In an equal volume ratio, 0.05 M pyrrole (98%, Merck, Germany), 0.05 M metandienone MD (Sigma-Aldrich) as a template molecule, and 0.1 M H₂SO₄ (98%, Sigma-Aldrich) were combined to make the electropolymerization electrolyte. The polypyrrole film was then oxidized using cyclic voltammetry (CV) in 0.1 M PBS (pH = 7.0) in a potential range of -0.15 to 1.1 V with a scanning rate of 20 mV/s for 5 cycles. Finally, the electrode was thoroughly rinsed with deionized water and immersed in 0.05 M oxalic acid dehydrate (99%, Sigma-Aldrich) for 30 minutes to remove the template molecules from the polypyrrole film.

2.2. Characterization

Amperometry and differential pulse voltammetry (DPV) measurements were performed using an electrochemical workstation potentiostat (RRDE-6A, Taizhou Hervey Instrument Co., Ltd., Jiangsu, China). All electrochemical measurements were performed in a 0.1M phosphate buffer solution (PBS) electrolyte (pH 7.0) prepared from a 0.1M NaH₂PO₄ (99%) and 0.1M Na₂HPO₄ (99%) mixture. The morphological and crystallographic properties of the nanostructures were evaluated using field emission scanning electron microscopy (FE-SEM) and an X-ray diffractometer (XRD, X'Pert-Pro-MRPD; Philips (Panalytical), Tokyo, Japan).

2.3. Preparation of the actual sample from the urine of wrestlers

To test the MIP/GO/GCE as a sensing system for MD analysis in real samples, urine samples from four wrestlers were provided. The wrestlers were given a placebo Dianabol injection (40 mg/ml, BioMed, UK) with an active half-life of 3-6 hours. Thus, urine samples were collected 2 hours after the Dianabol injection. The urine samples were centrifuged for 5 minutes at 1000 rpm, filtered, and then used to prepare 0.1 M PBS (pH 7.0). Finally, the 0.1 M PBS prepared from urine samples was used as an electrochemical electrolyte.

3. RESULTS AND DISCUSSION

3.1. Structural and morphological studies of modified electrodes

Figure 1 shows FE-SEM micrographs of modified electrodes (GO/GCE and MIP/GO/GCE). Figure 1a shows a FE-SEM micrograph of GO/GCE with laminated and overlapping flake nanosheets on the surface, which has a fairly irregular surface that is thin, wrinkled, and typically curved. The FE-SEM micrograph of MIP/GO/GCE (Figure 1b) shows that after electropolymerization, MIP nanoparticles can be evenly dispersed on the nanosheet surface of GO, forming new rough-shaped nanocomposite. Oxygen-containing functional groups on GO nanosheets, such as carboxyl and carbonyl, generate polymerization sites and a high degree of cross-linking [31-33].

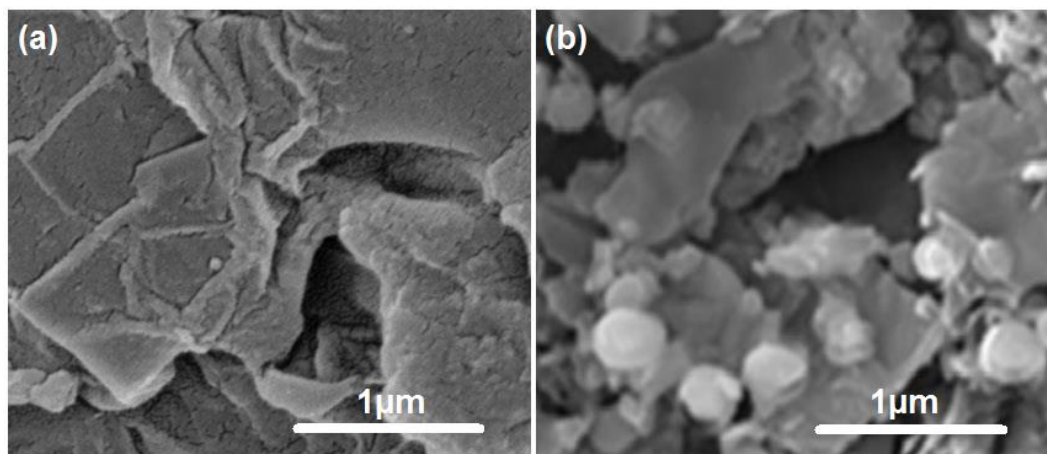


Figure 1. FE-SEM micrographs of modified electrodes: (a) GO/GCE and (b) MIP/GO/GCE.

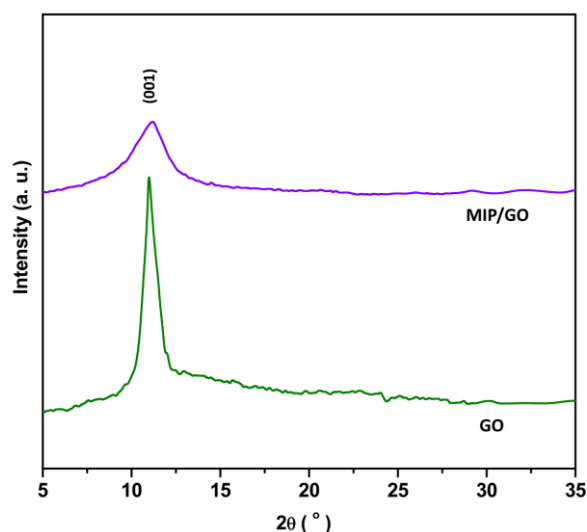


Figure 2. The results of structural characterization of powders of GO and MIP/GO nanocomposite by XRD.

Figure 2 depicts the results of the structural characterization of GO and MIP/GO nanocomposite powders. The XRD pattern of GO corresponds to a characteristic diffraction peak at 10.88° , which is assigned to the (001) Bragg reflection plane of the hexagonal structure of CNTs [34]. The same diffraction peak of the (001) crystalline plane can be seen in the XRD pattern of MIP/GO nanocomposite, but with a lower intensity [35, 36]. It was proposed that successful electropolymerization of MIP on GO nanosheets could improve adsorption and conductivity functionality [37, 38].

3.2. Electrochemical measurements

Figure 3 shows the DPV curves of MIP/GO/GCE, GO/GCE, and GCE at a scanning rate of 40 mV/s for a potential range of 0.20 to 1.25 V vs. Ag/AgCl in 0.1 M PBS at pH 7.0. The DPV

measurements were carried out in the electrochemical cell in both the absence and presence of MD solutions. In the absence of MD solution, none of the electrodes show a clear peak in the DPV curves. Following the addition of the MD solution, there are anodic peaks at 0.62 V, 0.66 V, and 0.72 V on the DPV curves of MIP/GO/GCE, GO/GCE, and GCE, respectively, which correspond to the suggested electrochemical oxidation process shown in Figure 4 [21]. Gómez et al. [39] also suggested that MD (17 β -hydroxy-17-methyl-1,4-androstadien-3-one) can be oxidized under oxidation of 17-hydroxyl group to 18-nor-17 β -hydroxymethyl-17 α -methylandrost-1,4,13-triene-3-one. Furthermore, Figure 3 shows that the DPV peak current of MIP/GO/GCE is greater than that of GO/GCE and unmodified GCE, and that the anodic peak is located at a significantly lower positive potential. It demonstrates that the synergistic effect of GO and MIPs significantly improves the electrocatalytic activity of MIP/GO nanocomposite [40]. The 2D structure of GO nanosheets with high conductivity, large surface area, and electrocatalytic activity can act as a suitable support for the immobilization of MIP molecules in sensor design and serve as a fast electron-transfer-shuttle in electrochemical reactions, increasing sensitivity [41-43]. MIPs electropolymerize to form 3D complementary cavities of a specific size and shape for the recognition of analyte molecules. These MIPs have a special place for specific analyte detection, as well as molecular recognition and catalysis mimics, and are capable of selectivity toward a target intrinsic template molecule [44-46]. Therefore, further electrochemical tests were conducted on MIP/GO/GCE.

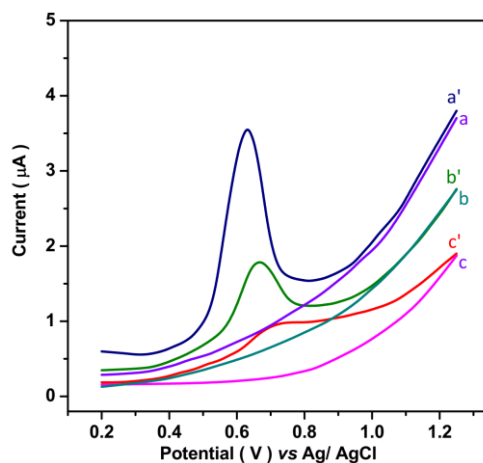


Figure 3. The DPV curves of unmodified (a and a') MIP/GO/GCE, (b and b') GO/GCE and (c and c') GCE at scanning rate of 40 mV/s for a potential range from 0.20 to 1.25 V vs. Ag/AgCl in 0.1 M PBS of pH 7.0 with and without MD solution.

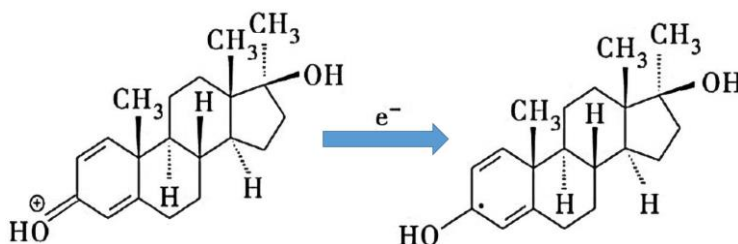


Figure 4. The suggested electrochemical oxidation process of MD [21].

Figure 5a shows the data obtained from amperometric measurements of MIP/GO/GCE using successive injections of a solution containing 100 ng/mL of MD solution in a 0.1 M PBS (pH 7.0) electrolyte solution at an applied potential of 0.62 V.

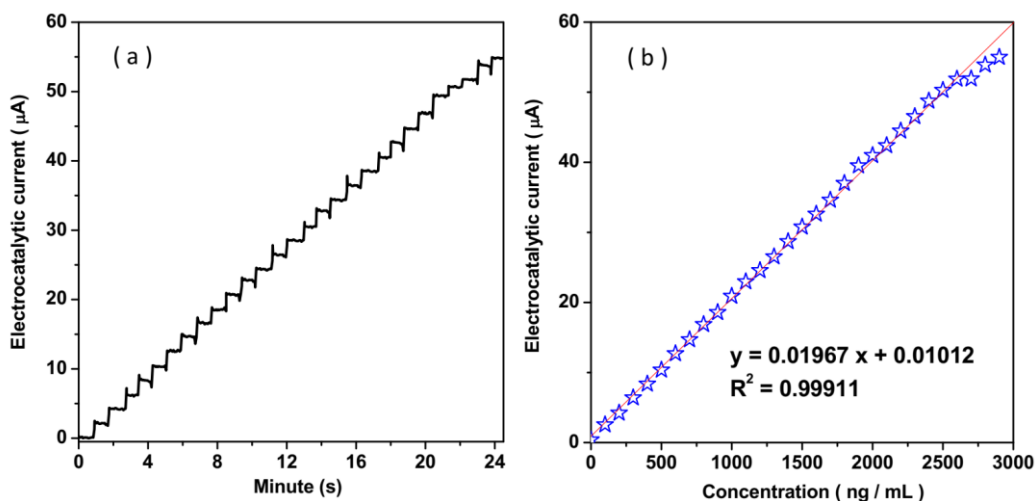


Figure 5. (a) The obtained data from amperometric measurements and (b) calibration graph of MIP/GO/GCE through successive injections of a solution containing 100 ng/mL MD solution in 0.1 M PBS (pH 7.0) electrolyte solution at an applied potential of 0.62 V.

Table 1. The performance of electrochemical sensor for determination of MD in present work and released outcomes of MD sensors in literatures.

Electrode	Technique	LOD (ng/ml)	Linear range (ng/ml)	Ref.
MIP/GO/GCE	Amperometry	0.07	0 – 2900	Present work
Carboxylated MWCNTs/Nafion/ GCE	DP-SCV	1	3 – 2704	[20]
o-phenylenediamine/Pt NPs/Au NWs/ ionic liquid	DPV	0.12	0.6 – 2884	[21]
Electrochemically reduced GO/GCE	DP-ASV	69.10	---	[22]
C18 SPE column	Capillary electrophoresis	4.5	0.2 – 2.0	[15]
HP-1 column	GC-LRMS-SIM	3	0.1 – 10	[17]
HP5-MS capillary column	LC-MS/MS	0.002	0.002 – 0.5	[18]
Ab-IgG-HRP/D-Bol-BAS/SPE	ELISA	0.6813	0 – 1000	[19]

DP-SCV: Differential pulse cathodic stripping voltammetry; DP-ASV: Differential pulse anodic square wave voltammetry; Ab-IgG-HRP/D-Bol-BAS/SPE: Anti-species IgG-HRP/boldenone-bovine serum albumin/Screen printed electrode

The results show that the MIP/GO/GCE responds quickly and sensitively to each addition of the MD solution. By increasing the MD concentration in an electrochemical cell, the amperometric current increases linearly. Figure 5b shows a calibration graph with a linear response from 0 to 2900 ng/mL. The sensitivity of MIP/GO/GCE is obtained to be $0.01967 \mu\text{A}/\text{ng}\cdot\text{mL}^{-1}$. limit of detection (LOD) can be determined according to the equation $\text{LOD} = 3\sigma/S$, where S is the slope of the calibration curve and σ is the standard deviation of blank solutions [47, 48]. The LOD is calculated to be 0.07 ng/mL. Table 1 shows that MIP/GO/GCE exhibits significant electrocatalytic performance with a broad linear range of MD concentrations and an appropriate LOD value when compared to the released outcomes of MD sensors in literatures. It may be related to grafting MIP molecules onto the surface of GO layers in order to increase surface area and improve sensing performance [49-51].

Table 2. The obtained data from amperometric measurements of MIP/GO/GCE through successive injections of a solution containing 10 ng/mL MD and 100 ng/mL interference species solutions in 0.1 M PBS (pH 7.0) at an applied potential of 0.62 V.

Substance	Added (ng/mL)	Amperometric signal (μA) at 0.62 V	RSD
MD	10	0.1971	± 0.0033
Testosterone	100	0.0439	± 0.0020
Glutamic acid,	100	0.0426	± 0.0014
19-Nortestosterone	100	0.0345	± 0.0015
Boldenone	100	0.0261	± 0.0011
Stanozolol	100	0.0436	± 0.0017
Keto-testosterone	100	0.0253	± 0.0011
Methylboldenone	100	0.0244	± 0.0018
Progesterone	100	0.0320	± 0.0019
Clenbuterol	100	0.0341	± 0.0011
Methyltestosterone	100	0.0194	± 0.0012
β -Estradiol	100	0.0240	± 0.0012
α -Testosterone	100	0.0126	± 0.0013
Acetaminophen	100	0.0175	± 0.0010
Uric acid	100	0.0251	± 0.0014
Dehydroepiandrosterone	100	0.0222	± 0.0016
α -Nortestosterone	100	0.0304	± 0.0018
α -Boldenone	100	0.0201	± 0.0012
Keto-nortestosterone	100	0.0154	± 0.0010

Before evaluating the proposed method for determining D-Bol in human biological fluid samples, the specificity of the MIP/GO/GCE system was tested in the presence of various chemicals and medicines that were found in biological fluid samples as interference species. Table 2 shows the results of amperometric measurements of MIP/GO/GCE using successive injections of a solution containing 10 ng/mL MD and 100 ng/mL interference species solutions in 0.1 M PBS (pH 7.0) at an applied potential of 0.62 V. The results show that adding MD solution to an electrochemical cell produces a significant electrocatalytic signal, but adding interference species to the electrolyte solution has no effect on the electrocatalytic signal, indicating the high specificity of the MIP/GO/GCE system

for determining MD in biological fluids samples. This specificity is due to MIP, which is created by electropolymerizing functional monomers in the presence of a target analyte (template). After the template is removed from the polymer, cavities are formed with a molecular memory that mirrors the size and shape of the template and mimics the binding sites of the target analyte [52].

The MIP/GO/GCE sensing system was evaluated as a proposed sensing system for MD analysis in real samples prepared from the urine of four wrestlers. Figure 6 depicts the data obtained from amperometric measurements of MIP/GO/GCE at an applied potential of 0.62 V using successive injections of a solution containing 100 ng/mL MD in 0.1 M PBS (pH 7.0) prepared from the urine sample of the first wrestler (W1). The calibration graph in Figure 6b shows that the MD level in the processed sample is 5.23 ng/mL. This method was used to analyze the remaining samples (W2–W4), and the results are summarized in Table 3. As can be seen, the MD levels determined in urine samples are close to each other. In addition, the outcomes of analytical studies in Table 3 illustrate that the RSD values (3.15% to 4.73%) are appropriate for valid and accurate practical analyses in urine and other biological fluid samples.

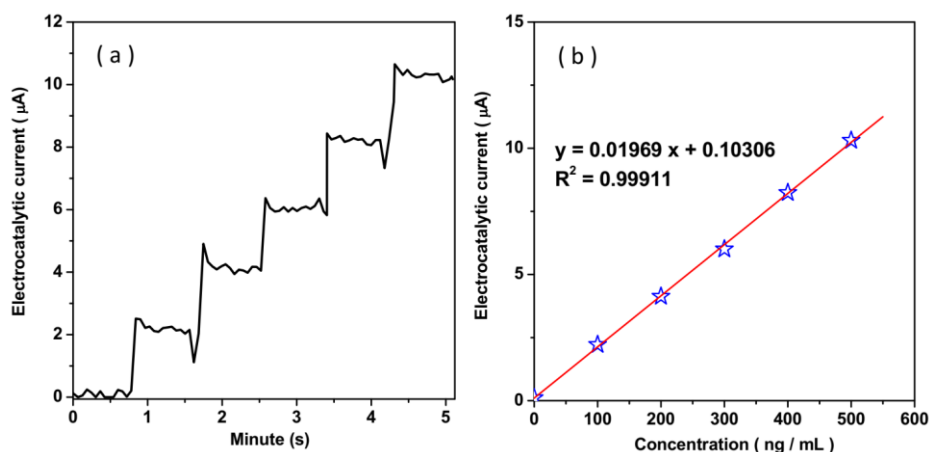


Figure 6. (a) The obtained data from amperometric measurements and (b) calibration graph of MIP/GO/GCE through successive injections of a solution containing 100 ng/mL MD in 0.1 M PBS (pH 7.0) prepared from urine sample of first wrestler (W1) at an applied potential of 0.62 V.

Table 3. The obtained data from amperometric measurements to determination of MD level in prepared real samples from wrestlers's urine samples undergoing administration injection of Dianabol.

Sample No.	Detected content of MD in prepared urine samples (ng/mL)	RSD (%)
W1	5.23	±3.73
W2	4.96	±4.58
W3	5.05	±4.22
W4	4.56	±3.15

4. CONCLUSION

In this paper, an electropolymerization technique was used to create a modified MIP/GO/GCE as an electrochemical sensor for the selective determination of MD in wrestlers' biological fluid samples. In the MIP/GO nanocomposite, structural and morphological studies confirmed the successful electropolymerization of MIP on GO nanosheets. Due to the synergistic effect of GO and MIPs, electrochemical measurements revealed highly selective MD determination and significantly enhanced electrocatalytic activity of the MIP/GO nanocomposite. The MIP/GO/GCE linear response was measured from 0 to 2900 ng/mL. The sensitivity and detection limit were calculated to be $0.01967\mu\text{A}/\text{ng}\cdot\text{mL}^{-1}$ and $0.07\text{ng}/\text{mL}$, respectively. Furthermore, when compared to the released results of MD sensors in literatures, MIP/GO/GCE demonstrated significant electrocatalytic performance with a broad linear range to MD concentrations and an appropriate limit of detection value. The MIP/GO/GCE sensing system was evaluated as a proposed sensing system for MD analysis in real samples prepared from the urine of four wrestlers. Analytical studies revealed that the RSD values were suitable for valid and accurate practical analyses in urine and other biological fluid samples.

References

1. S.M. Reitzner, J. Hengevoss, E. Isenmann and P. Diel, *The Journal of Steroid Biochemistry and Molecular Biology*, 190 (2019) 44.
2. H. Maleh, M. Alizadeh, F. Karimi, M. Baghayeri, L. Fu, J. Rouhi, C. Karaman, O. Karaman and R. Boukherroub, *Chemosphere*, (2021) 132928.
3. J.D. Wilson, *Endocrine reviews*, 9 (1988) 181.
4. T. Gao, C. Li, M. Yang, Y. Zhang, D. Jia, W. Ding, S. Debnath, T. Yu, Z. Said and J. Wang, *Journal of Materials Processing Technology*, 290 (2021) 116976.
5. V.R. Kozhuharov, K. Ivanov and S. Ivanova, *BioMed Research International*, 2022 (2022) 1.
6. Y. Chen, J. Long, B. Xie, Y. Kuang, X. Chen, M. Hou, J. Gao, H. Liu, Y. He and C.-P. Wong, *ACS Applied Materials & Interfaces*, 14 (2022) 4647.
7. A. Zschiesche, Z. Chundela, D. Thieme and A.M. Keiler, *Drug Testing and Analysis*, 14 (2022) 298.
8. B. Huang, L. Changhe, Y. Zhang, D. Wenfeng, Y. Min, Y. Yuying, Z. Han, X. Xuefeng, W. Dazhong and S. Debnath, *Chinese Journal of Aeronautics*, 34 (2021) 1.
9. Q. Yin, C. Li, L. Dong, X. Bai, Y. Zhang, M. Yang, D. Jia, R. Li and Z. Liu, *International Journal of Precision Engineering and Manufacturing-Green Technology*, 8 (2021) 1629.
10. F. Aknouche, L. Gueddar, A. Kernalleguen, C. Maruejouis and P. Kintz, *Toxicologie Analytique et Clinique*, 33 (2021) S15.
11. M. Yang, C. Li, L. Luo, R. Li and Y. Long, *International Communications in Heat and Mass Transfer*, 125 (2021) 105317.
12. H. Karimi-Maleh, R. Darabi, M. Shabani-Nooshabadi, M. Baghayeri, F. Karimi, J. Rouhi, M. Alizadeh, O. Karaman, Y. Vasseghian and C. Karaman, *Food and Chemical Toxicology*, 162 (2022) 112907.
13. D.Z. Stakic, D. Agbaba and S. Vladimirov, *Analytical letters*, 25 (1992) 1687.
14. W. Schänzer, H. Geyer, G. Fußhöller, N. Halatcheva, M. Kohler, M.K. Parr, S. Guddat, A. Thomas and M. Thevis, *Rapid communications in mass spectrometry*, 20 (2006) 2252.
15. B. Du, J. Zhang, Y. Dong, J. Wang, L. Lei and R. Shi, *Steroids*, 161 (2020) 108691.

16. I.V. Sych, O.V. Bevz, I.A. Sych, A.M. Shaposhnyk, M.V. Zarubina, O.V. Kryvanych, N.L. Bereznyakova, S.G. Taran and L.O. Perekhoda, *Research Journal of Pharmacy and Technology*, 14 (2021) 5169.
17. J. Kokkonen, A. Leinonen, J. Tuominen and T. Seppälä, *Journal of Chromatography B: Biomedical Sciences and Applications*, 734 (1999) 179.
18. M. Bresson, V. Cirimele, M. Villain and P. Kintz, *Journal of chromatography B*, 836 (2006) 124.
19. H. Lu, G. Conneely, M. Pravda and G.G. Guilbault, *Steroids*, 71 (2006) 760.
20. N.M. Alourfi, G.I. Mohammed, H.M. Nassef, H. Alwael, E.A. Bahaidarah, A.S. Bashammakh, L.H. Mujawar and M.S. El-Shahawi, *Analytical Sciences*, 1 (2021) 21P167.
21. L. Shan, *International Journal of Electrochemical Science*, 15 (2020) 12587.
22. N.X. Hung and N.N. Dung, *PalArch's Journal of Archaeology of Egypt/Egyptology*, 18 (2021) 4261.
23. W. Zheng, J. Cheng, X. Wu, R. Sun, X. Wang and X. Sun, *Knowledge-Based Systems*, 241 (2022) 108293.
24. T. Gao, Y. Zhang, C. Li, Y. Wang, Q. An, B. Liu, Z. Said and S. Sharma, *Scientific reports*, 11 (2021) 1.
25. L. Chen, X. Wang, W. Lu, X. Wu and J. Li, *Chemical Society Reviews*, 45 (2016) 2137.
26. Z. Zhang, Y. Li, X. Liu, Y. Zhang and D. Wang, *International journal of electrochemical science*, 13 (2018) 2986.
27. Z. Chen, Z. Hua, L. Xu, Y. Huang, M. Zhao and Y. Li, *Journal of Molecular Recognition: An Interdisciplinary Journal*, 21 (2008) 71.
28. L. Shi, J. Duan, S. Xu, H. Yang and G. Yang, *International Journal of Electrochemical Science*, 16 (2021) 210767.
29. S. Sun, M. Zhang, Y. Li and X. He, *Sensors*, 13 (2013) 5493.
30. M.d.L. Gonçalves, L.A. Truta, M.G.F. Sales and F.T. Moreira, *Analytical Letters*, 54 (2021) 2611.
31. X. Chen and N. Ye, *Rsc Advances*, 7 (2017) 34077.
32. X. Wei, X. Xu, W. Qi, Y. Wu and L. Wang, *Progress in Natural Science: Materials International*, 27 (2017) 374.
33. X.-Y. Li, Y. Song, C.-X. Zhang, C.-X. Zhao and C. He, *Separation and Purification Technology*, 279 (2021) 119608.
34. T.N. Blanton and D. Majumdar, *Powder Diffraction*, 27 (2012) 104.
35. S. Han, X. Li, Y. Wang and C. Su, *Analytical Methods*, 6 (2014) 2855.
36. M. Liu, C. Li, Y. Zhang, Q. An, M. Yang, T. Gao, C. Mao, B. Liu, H. Cao and X. Xu, *Frontiers of Mechanical Engineering*, 16 (2021) 649.
37. M.A. Beluomini, J.L. da Silva, A.C. de Sá, E. Buffon, T.C. Pereira and N.R. Stradiotto, *Journal of Electroanalytical Chemistry*, 840 (2019) 343.
38. Z. Duan, C. Li, W. Ding, Y. Zhang, M. Yang, T. Gao, H. Cao, X. Xu, D. Wang and C. Mao, *Chinese journal of mechanical engineering*, 34 (2021) 1.
39. C. Gómez, O. Pozo, L. Garrostas, J. Segura and R. Ventura, *Steroids*, 78 (2013) 1245.
40. Y. Wang, C. Li, Y. Zhang, M. Yang, B. Li, L. Dong and J. Wang, *International Journal of Precision Engineering and Manufacturing-Green Technology*, 5 (2018) 327.
41. S. Alexander, P. Baraneedharan, S. Balasubrahmanyam and S. Ramaprabhu, *Materials Science and Engineering: C*, 78 (2017) 124.
42. Z. Savari, S. Soltanian, A. Noorbakhsh, A. Salimi, M. Najafi and P. Servati, *Sensors and Actuators B: Chemical*, 176 (2013) 335.
43. H. Savaloni, E. Khani, R. Savari, F. Chahshouri and F. Placido, *Applied Physics A*, 127 (2021) 1.

44. S.E. Elugoke, A.S. Adekunle, O.E. Fayemi, E.D. Akpan, B.B. Mamba, E.S.M. Sherif and E.E. Ebenso, *Electrochemical Science Advances*, 1 (2021) e2000026.
45. F. Zhao, S. Zhang, Q. Du, J. Ding, G. Luan and Z. Xie, *Socio-Economic Planning Sciences*, 78 (2021) 101066.
46. H. Karimi-Maleh, C. Karaman, O. Karaman, F. Karimi, Y. Vasseghian, L. Fu, M. Baghayeri, J. Rouhi, P. Senthil Kumar and P.-L. Show, *Journal of Nanostructure in Chemistry*, (2022) 1.
47. M. Xie, Z. Chen, F. Zhao, Y. Lin, S. Zheng and S. Han, *Foods*, 11 (2022) 1933.
48. H. Karimi-Maleh, H. Beitollahi, P.S. Kumar, S. Tajik, P.M. Jahani, F. Karimi, C. Karaman, Y. Vasseghian, M. Baghayeri and J. Rouhi, *Food and Chemical Toxicology*, (2022) 112961.
49. W. Liu, Y. Ma, G. Sun, S. Wang, J. Deng and H. Wei, *Biosensors and Bioelectronics*, 92 (2017) 305.
50. R. Savari, J. Rouhi, O. Fakhar, S. Kakooei, D. Pourzadeh, O. Jahanbakhsh and S. Shojaei, *Ceramics International*, 47 (2021) 31927.
51. H. Savaloni, R. Savari and S. Abbasi, *Current Applied Physics*, 18 (2018) 869.
52. A. Yarman and F.W. Scheller, *Sensors*, 20 (2020) 2677.

© 2022 The Authors. Published by ESG (www.electrochemsci.org). This article is an open access article distributed under the terms and conditions of the Creative Commons Attribution license (<http://creativecommons.org/licenses/by/4.0/>).